European Journal of Radiology 83 (2014) e137–e146

Contents lists available at ScienceDirect

European Journal of Radiology

journal homepage: www.elsevier.com/locate/ejrad

Review

CT and MR imaging findings of palatal tumors

Hiroki Kato[a,*], Masayuki Kanematsu[a,b,1,2], Hiroki Makita[c,1], Keizo Kato[c,1], Daijiro Hatakeyama[c,1], Toshiyuki Shibata[c,1], Keisuke Mizuta[d,1], Mitsuhiro Aoki[d,1]

[a] Department of Radiology, Gifu University School of Medicine, 1-1 Yanagido, Gifu 501-1194, Japan
[b] High-level Imaging Diagnosis Center, Gifu University Hospital, 1-1 Yanagido, Gifu 501-1194, Japan
[c] Department of Oral and Maxillofacial Sciences, Gifu University School of Medicine, Gifu, Japan
[d] Department of Otolaryngology, Gifu University School of Medicine, Gifu, Japan

ARTICLE INFO

Article history:
Received 23 August 2013
Received in revised form
26 November 2013
Accepted 27 November 2013

Keywords:
Palate
Tumor
Hard palate
Soft palate
CT
MRI

ABSTRACT

Palatal tumors commonly arise from the minor salivary glands, and benign tumors account for approximately half of all minor salivary gland tumors. Minor salivary gland tumors have an affinity for the posterior hard palate and soft palate and virtually never arise in the midline, probably because of the distribution of palatal salivary glands. The majority of benign salivary gland tumors of the palate are pleomorphic adenomas, while the most common malignant salivary gland tumor is adenoid cystic carcinoma, followed by mucoepidermoid carcinoma, adenocarcinoma, and polymorphous low-grade adenocarcinoma. Epithelial tumors frequently arise from the soft palate. The majority of benign epithelial tumors of the palate are papillomas, while most malignant epithelial tumors are squamous cell carcinomas. Various types of mesenchymal tumors, including fibromas, lipomas, schwannomas, neurofibromas, hemangiomas, and lymphangiomas, also involve the palate. This article describes the CT and MR findings of benign and malignant palatal tumors.

1. Introduction

The hard palate is one of the anatomical subdivisions of the oral cavity. It comprises the anterior two-thirds of the palate and separates the oral cavity from the nasal cavity. It is formed by the palatine process of the maxilla and the horizontal plate of the palatine bone, which is covered by a mucous membrane, and hundreds of minor salivary glands are located between the mucosal surface and the underlying bone.

The soft palate is one of the anatomical subdivisions of the oropharynx. It comprises the posterior third of the palate and separates the oropharynx from the nasopharynx. It is formed by connective tissue and muscle fibers, mainly the glossopalatine and pharyngopalatine muscles, without underlying bone. The soft palate is covered by squamous mucosa and contains a smaller number of minor salivary glands compared with the hard palate. It is very flexible during speaking and swallowing.

Minor salivary glands usually located in the oral cavity, include the labial, buccal, molar, lingual, and palatine glands. The palatine glands form a thick submucosal layer in the soft palate and a thin submucosal layer in the hard palate, but they are absent in the region of the incisive fossa and the anterior part of the palatine raphe. The palatine glands are primarily mucous secreting glands.

The sensory supply to the palate is derived mainly from branches of the maxillary nerve via the pterygopalatine ganglion in the pterygopalatine fossa. The greater palatine nerve exits to the oral cavity via the greater palatine foramen, whereas the lesser palatine nerve via the lesser palatine foramen (Fig. 1). The nasopalatine nerve passes along the nasal septum in the nasal cavity, and into palatal mucosa through the incisive foramen. The greater palatine nerve supplies the gums, the mucosa and glands of the hard palate, and communicates in front with the nasopalatine nerve, whereas the lesser palatine nerve supplies the mucosa and glands of the soft palate and uvula. A small area behind the incisor teeth is supplied by the nasopalatine nerves.

From the pterygomaxillary junction to the pterygopalatine fossa region, the maxillary artery was usually branched into 5 arteries in the following order: posterior superior alveolar artery, infraorbital artery, artery of the pterygoid canal, descending palatine artery, and sphenopalatine artery. The descending palatine artery branches into the greater palatine artery and lesser palatine artery. The greater palatine artery descends through the greater palatine foramen and supplies the hard palate, anastomosing through the

* Corresponding author. Tel.: +81 58 230 6439; fax: +81 58 230 6440.
E-mail addresses: hkato@gifu-u.ac.jp (H. Kato), masa_gif@yahoo.co.jp (M. Kanematsu), makitah@gifu-u.ac.jp (H. Makita), keizo@gifu-u.ac.jp (K. Kato), hatakeya@gifu-u.ac.jp (D. Hatakeyama), shibat@gifu-u.ac.jp (T. Shibata), kmizuta@gifu-u.ac.jp (K. Mizuta), aoki@gifu-u.ac.jp (M. Aoki).
[1] Tel.: +81 58 230 6439; fax: +81 58 230 6440.
[2] Tel.: +81 58 230 6000; fax: +81 58 230 6080.

0720-048X/$ – see front matter © 2013 Elsevier Ireland Ltd. All rights reserved.
http://dx.doi.org/10.1016/j.ejrad.2013.11.028

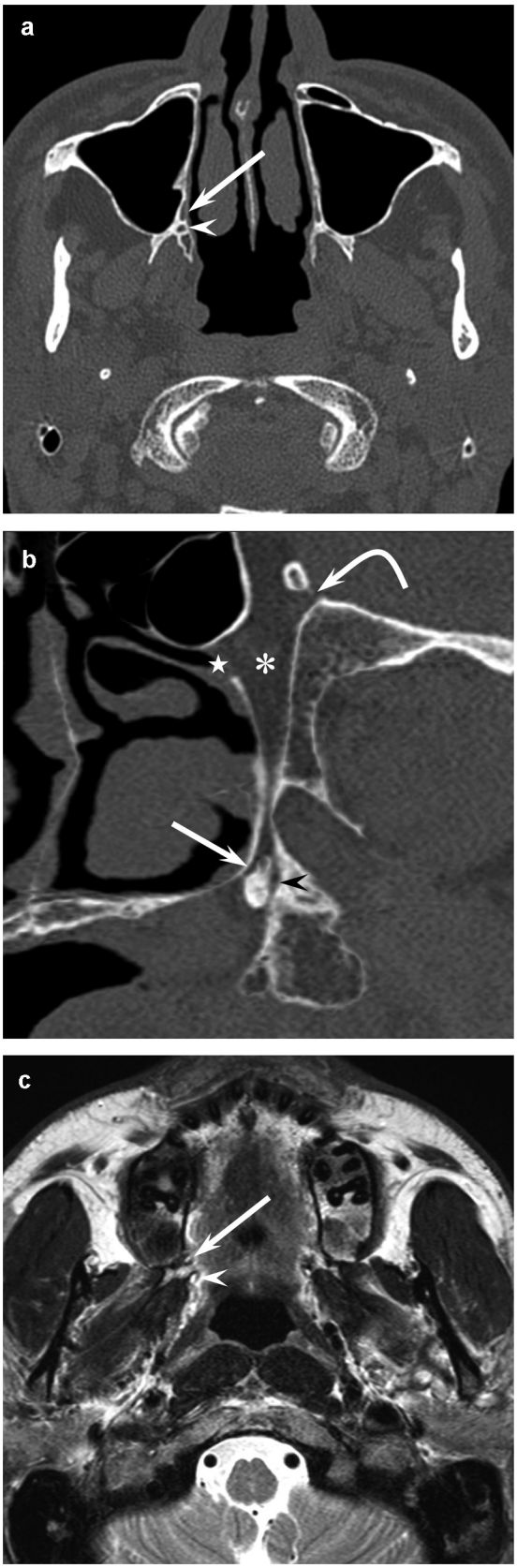

Fig. 1. A 38-year-old man with normal palatal anatomy. (a) Axial CT image shows greater (arrows) and lesser (arrow heads) palatine foramen. (b) Oblique sagittal reformatted CT image shows pterygopalatine fossa (asterisk) that connects with greater (arrows) and lesser (arrow heads) palatine foramen, sphenopalatine foramen (star), and round foramen (curved arrow). (c) Axial T2-weighted image shows greater (arrows) and lesser (arrow heads) palatine foramen.

incisive foramen with the posterior septal branches of sphenopalatine artery that supplies the nasal cavity. The lesser palatine artery descends through the lesser palatine foramen and supplies the soft palate and the palatine tonsils, anastomosing with the ascending palatine artery that branches off from the facial artery.

Benign and malignant palatal tumors are usually asymptomatic masses that are occasionally associated with a low level of discomfort. Salivary gland tumors of the palate usually appear as slow-growing, well-circumscribed, dome-shaped, smooth-surfaced, nonmovable swellings. Pain or ulceration is occasionally observed. Adjacent bone invasion, perineural extension, and sinonasal involvement are commonly observed with palatal malignancies [1]. Tumor size, histological tumor grade, and presence of lymph node metastasis at the time of initial diagnosis are associated prognostic factors for palatal malignancies [2,3].

Preoperatively, fine-needle aspiration cytology plays a definitive role in revealing the epithelial, myoepithelial, and stromal components of tumors [4]. CT and MR imaging are usually performed to assess the extent of the tumor, including bone erosion or destruction, soft tissue involvement, and perineural spread. This review aims to illustrate the CT and MR imaging findings of benign and malignant palatal tumors.

2. Cross-sectional imaging

CT and MR imaging are the most frequently used imaging modalities. CT is useful for evaluating adjacent bone erosion or destruction, and coronal CT images should be obtained by multiplanar reconstruction (MPR). Metallic artifacts are quite common in CT images of patients who have metallic dental implants or filling materials, whereas most dental metallic materials usually cause mild distortions to the local magnetic field. Moreover, MR imaging provides excellent soft-tissue contrast that is considerably superior to that of CT. Therefore, MR imaging can allow the assessment of differential diagnosis and tumor extent. MR imaging is also more sensitive than CT in the detection of perineural spread, and it is preferable to obtain the contrast-enhanced fat-suppressed T1-weighted MR images for the evaluation of perineural spread. However, some authors suggest that the sequence should be non-fat-suppressed due to susceptibility artifacts of the fat suppressed sequences [5].

3. Staging of malignant palatal tumors

Malignancies of hard or soft palate origin are known to spread perineurally along the palatine branches of the maxillary nerve. The characteristic imaging findings of perineural spread into greater or lesser palatine foramen include asymmetric enlargement or destruction on CT images, obliteration of fat plane on T1-weighted images, or the enlarged nerves with abnormal enhancement on contrast-enhanced T1-weighted fat-suppressed MR images.

Malignancies of soft palate occasionally metastasise to cervical lymph nodes in level II, followed by level III. CT and MR images can characterize cervical nodes according to morphological criteria (size, configuration, hilum, necrosis, and extracapsular spreading). Although the size of the lymph node is most frequently used for differential diagnosis, the accuracy of this criterion is insufficient. The detection of nodal necrosis in patients with head and neck malignancies is the most reliable indication of metastatic nodes. Although CT was considered the best technique for detecting nodal necrosis before the year 2000 [6,7], recent advanced technologies can produce high-quality MR images with the potential to improve the diagnostic accuracy for nodal necrosis [8,9]. Contrast-enhanced CT and MR images are required to improve the detection of nodal necrosis.

4. Benign tumors

4.1. Pleomorphic adenoma

Pleomorphic adenoma is the most common type of salivary gland tumor of the palate. Other sites of occurrence in the oral cavity include the lips, buccal mucosa, tongue, floor of the mouth, tonsils, pharynx, and retromolar area [10]. In the palate, it is commonly located lateral to the midline of the posterior hard palate. These tumors frequently present as painless, firm or rubbery, slow-growing, well-delineated masses that are covered with normal mucous membranes, although mucosal ulcerations are occasionally observed [11]. These tumors may be accompanied by discomfort while chewing or difficulty while speaking.

Pleomorphic adenoma of the palate occasionally invades or erodes the adjacent bone (Fig. 2a) [12]. On MR images, the borders of parotid and submandibular gland lesions often show lobulation, while those of palatal lesions are usually smooth [13]. Fibrous capsules appearing as hypointense on T2-weighted images are rather characteristic of pleomorphic adenoma (Fig. 2b). The characteristic enhancement pattern of pleomorphic adenoma is delayed enhancement, increasing in both degree and homogeneity with time [14].

4.2. Myoepithelioma

Myoepithelioma, also known as myoepithelial adenoma or benign myoepithelial tumor, is a rare tumor of myoepithelial differentiation that accounts for 1.5% of all salivary gland tumors. The most common site of occurrence is the parotid gland, followed by the minor salivary glands in the oral cavity. The palate is the most common site of origin of intraoral myoepithelioma [15]. These tumors usually present as asymptomatic masses and grow slowly over a period of several months or years [16].

Parotid gland myoepithelioma presents as a well-circumscribed mass with smooth or lobulated margins [17]. Homogeneous or heterogeneous enhancement is observed, and various degrees of enhancement are observed in accordance with the histological components [15]. Palatal lesions also present as well-demarcated masses, and adjacent bone erosion may be observed [18]. Palatal lesions show hypointensity on T1-weighted images and hyperintensity on T2-weighted images (Fig. 3) [19]. Radiological differentiation of myoepithelioma from other salivary gland tumors such as pleomorphic adenoma may be difficult.

4.3. Papilloma

Papilloma, also referred to as squamous papilloma, is a benign epithelial tumor composed of fingerlike projections of squamous epithelium, and it commonly occurs in the oral cavity and oropharynx [20]. The soft palate is the most common site for oral cavity lesions, accounting for 20% of all lesions, followed by the uvula, tongue, lips, and gingiva [20]. Papillomas usually appear as pedunculated or sessile, white or normal-colored, cauliflower-like projections that arise from the mucosal surface. Human papilloma virus (HPV) subtypes 6 and 11 have been identified in up to 50% of oral papillomas [21].

CT and MR images are useful for assessing the size and shape of lesions and evaluating the presence of tumor invasion. Papillomas appear as well-defined, polypoid lesions that are occasionally accompanied by stalks (Fig. 4). Although the configuration of the papillary projection is characteristic, it is often difficult to differentiate these tumors from other nonepithelial or mesenchymal tumors.

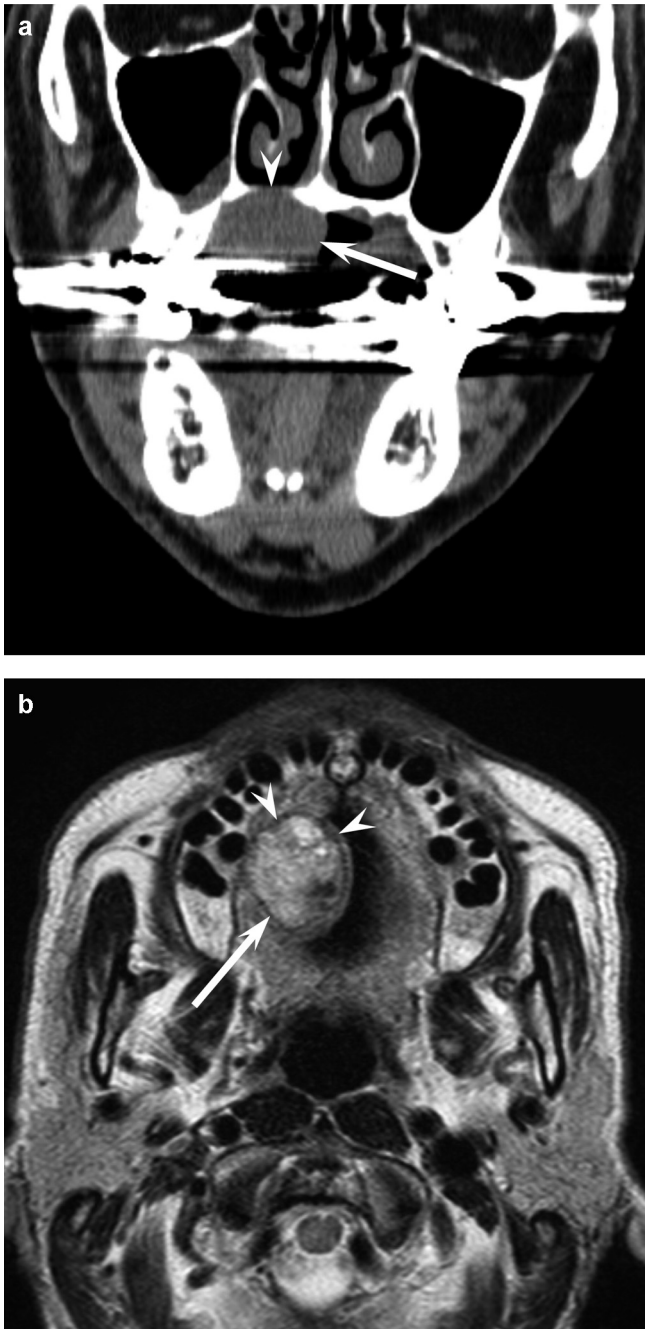

Fig. 2. A 60-year-old man with pleomorphic adenoma of the right hard palate. (a) Coronal reformatted unenhanced CT image shows a hypodense lesion (arrow) with bone erosion of adjacent hard palate (arrow head). (b) Axial T2-weighted image shows a well-demarcated, heterogeneous, hyperintense lesion (arrow) with fibrous capsule (arrow heads).

4.4. Schwannoma

Schwannoma is a benign tumor that originates from peripheral nerve Schwann cells. These tumors often arise in the head and neck region but are rarely found in the oral cavity. The most frequent site within the oral cavity is the tongue, followed by the buccal mucosa, palate, floor of the mouth, gingiva, and lips [22]. Because schwannomas usually present as painless, firm, slow-growing, well-delineated masses with smooth surfaces, patients with these tumors experience a long course of illness and present with larger tumors at initial diagnosis.

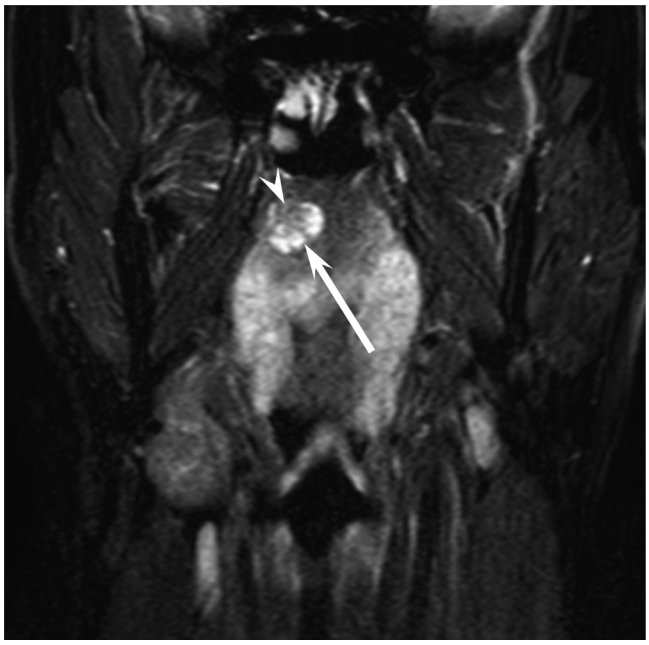

Fig. 3. A 37-year-old man with myoepithelioma of the right soft palate. Coronal fat-suppressed T2-weighted images shows a heterogeneously hyperintense lesion (arrow) with internal hypointense areas (arrow head).

On MR images, schwannomas usually present as fusiform masses accompanied by entering and exiting nerves and surrounding fibrous capsules. Palatal schwannomas present as well-demarcated masses with adjacent bone erosion [23]. Intratumoral degenerative changes are thought to result from long-term progression, and microhemorrhage is considered to be a mechanism of cyst formation [24].

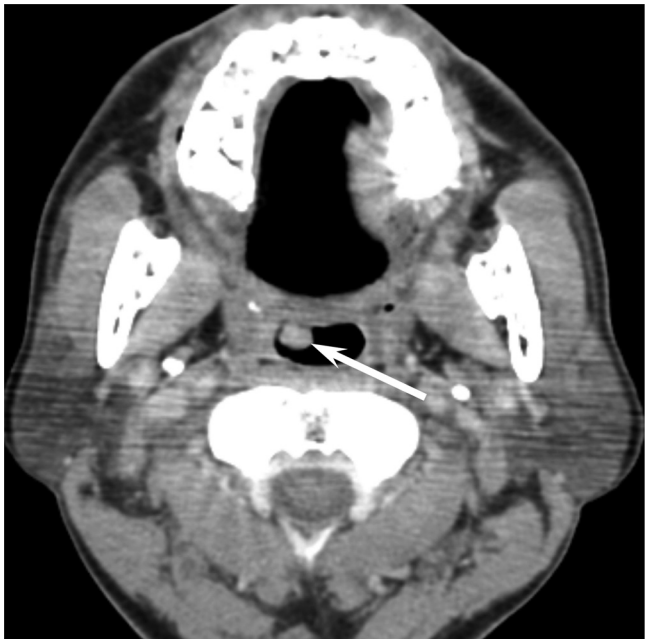

Fig. 4. A 62-year-old man with papilloma of the right soft palate. Axial enhanced CT image shows a well-demarcated, polypoid, homogeneously enhanced lesion (arrow).

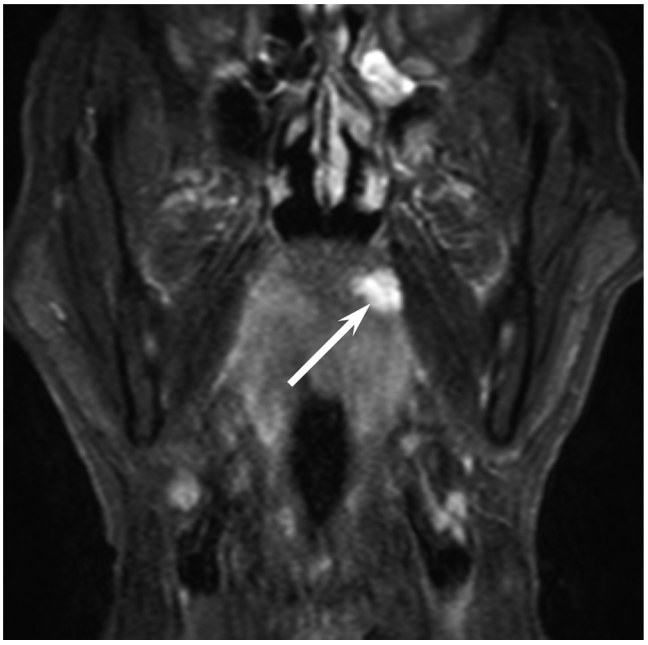

Fig. 5. A 67-year-old man with cavernous hemangioma of the left soft palate. Coronal fat-suppressed T2-weighted image shows a well-demarcated, lobulated, homogeneous, intensely hyperintense lesion (arrow).

4.5. Hemangioma

Vascular anomalies are classified as infantile hemangiomas and vascular malformations [25]. Infantile hemangioma is a benign vascular tumor that presents a clinical course characterized by early proliferation and subsequent spontaneous involution. Vascular malformations are subclassified as capillary, venous, lymphatic, and arteriovenous types. Vascular anomalies rarely occur in the oral cavity, but they can arise from the tongue, lips, buccal mucosa, gingiva, and palate [26]. These anomalies appear as soft, deep red-colored, smooth or lobulated, sessile or pedunculated masses of various sizes and may interfere with mastication [26].

Phleboliths are calcified nodules that are regarded as characteristic properties of venous malformation and are also referred to as cavernous hemangiomas. On T2-weighted images, cavernous hemangiomas generally appear as multiple hyperintense lobules that resemble a bunch of grapes (Fig. 5). Punctate or reticular hypointense areas may be present, representing fibrous tissue, fast flow within vessels, or calcified foci [27]. The presence of fluid–fluid level suggests the separation of blood cells and serous fluid due to the extremely slow flow in cavernous hemangioma.

4.6. Pyogenic granuloma (lobular capillary hemangioma)

Pyogenic granuloma, also known as lobular capillary hemangioma, is a benign vascular lesion that affects the skin and mucous membranes [28]. Trauma and local irritation are thought to be major causes, and poor oral hygiene may be a predisposing factor. Intraoral pyogenic granulomas show a striking predilection for gingival and interdental papilla involvement, but extragingival lesions can occasionally occur in the lower lip, tongue, and palate [29]. These tumors are typically small, polypoid lesions that are often ulcerated and friable. Pyogenic granulomas often have an initial period of rapid growth, followed by stabilization and occasionally regression.

Although CT and MR imaging features of palatal pyogenic granulomas have not been previously reported, these features have been described in lesions involving other locations such as the nasal

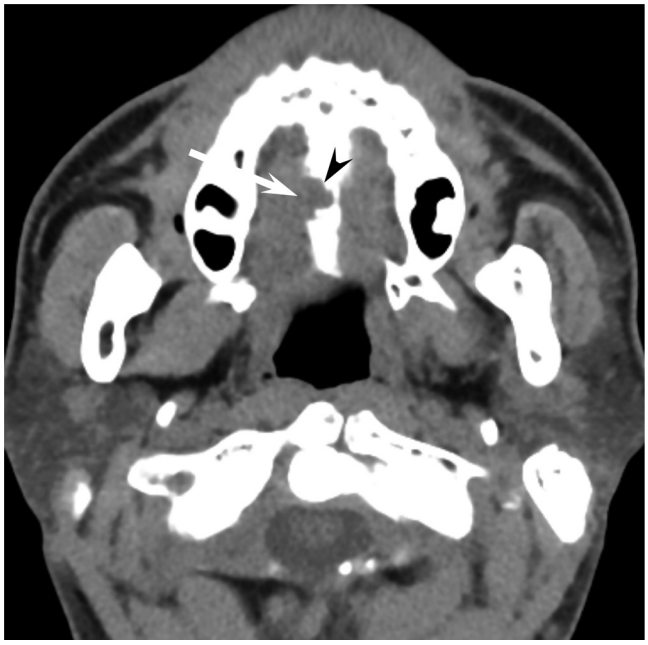

Fig. 6. A 38-year-old man with pyogenic granuloma of the right hard palate. Axial unenhanced CT image shows a hypodense lesion (arrow) with bone erosion of adjacent hard palate (arrow head).

cavity and finger. These lesions have appeared as hypointense on T1-weighted images and hyperintense on T2-weighted images, and shown intense enhancement due to their vascular nature (Fig. 6) [28,30].

4.7. Fibroma

Fibroma, also referred to as irritation fibroma, is a painless, localized, slow-growing, fibroblastic proliferation arising from the oral mucosa. While this terminology implies a benign neoplasm, fibromas usually present as reactive fibrous hyperplasia caused by trauma and local irritation. Although these lesions may occur at any oral site, they are frequently observed in the buccal mucosa along the occlusal surface. Other common sites include the tongue, gingiva, and lower lip. Fibromas are asymptomatic, round-to-ovoid, smooth-surfaced, sessile or pedunculated masses that are usually <1 cm in size, although these lesions can increase to >3 cm in size.

CT and MR findings of oral fibromas have not been previously described. In our case, T2-weighted images showed a hyperintense mass accompanied by peripheral hypointense areas that corresponded to fibrous tissue (Fig. 7a). Moderate and weak levels of enhancement were observed in the central and peripheral areas, respectively (Fig. 7b).

4.8. Exostosis (torus palatinus)

Torus palatinus is a benign developmental exostosis that arises from the midline of the hard palate. These tumors are categorized according to their configuration and can be classified as flat, nodular, lobular, or spindle types [31]. Torus palatinus is asymptomatic in most patients, but mucosal ulcerations can develop from repeated trauma. A mandibular counterpart is referred to as torus mandibularis.

Torus palatinus clearly appears as a bony protuberance arising from the inferior surface of the hard palate on coronal and sagittal CT images (Fig. 8a), while a lobulated appearance may be better observed on axial CT images (Fig. 8b). These tumors usually comprise compact bone with homogeneous mineralization, but some cases contain bone marrow and present with trabeculations [32].

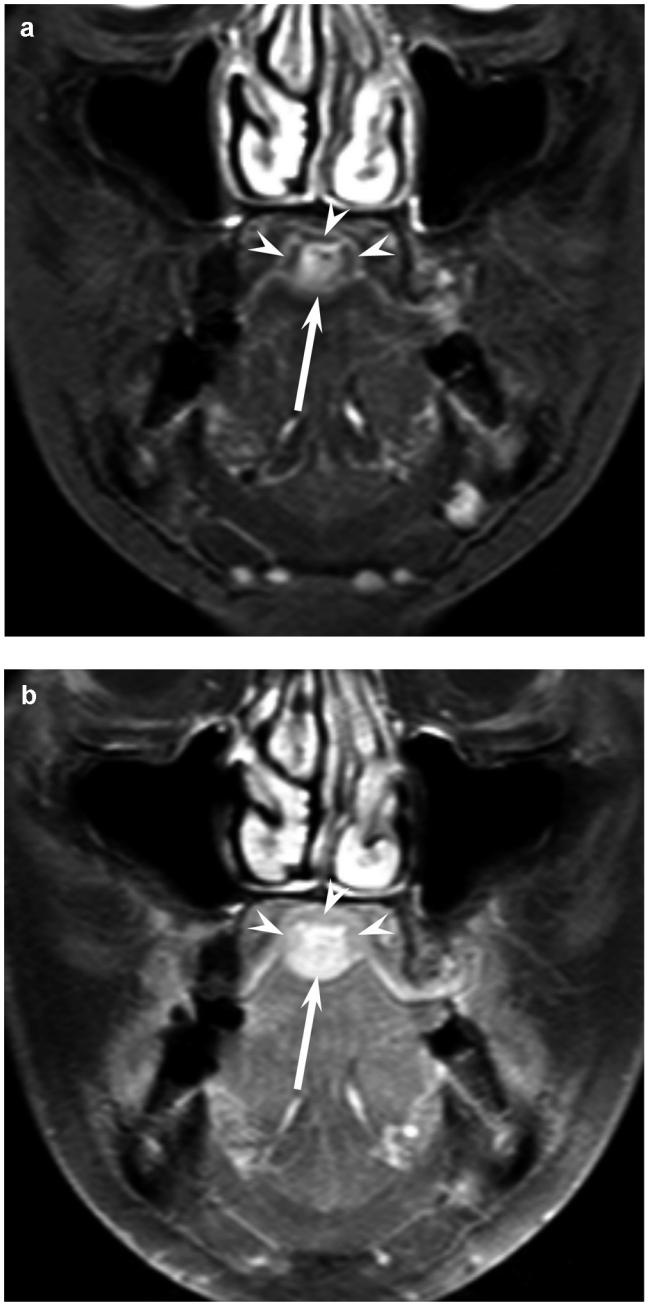

Fig. 7. A 49-year-old woman with fibroma of the right hard palate. (a) Coronal fat-suppressed T2-weighted image shows a well-demarcated, heterogenous, hyperintense lesion (arrow) with hypointense areas in the periphery (arrow heads). (b) Coronal gadolinium-enhanced fat-suppressed T1-weighted image shows a enhanced lesion (arrow) with weakly enhanced areas in the periphery (arrow heads).

4.9. Fibrous dysplasia

Fibrous dysplasia is considered to be a developmental skeletal disorder characterized by the replacement of normal bone with cellular fibrous connective tissue. These dysplasias are classified into the monostotic and polyostotic forms. Common sites of the monostotic form include the ribs, femurs, and craniofacial bones. Craniofacial lesions most commonly involve the facial bones and the skull base. The major symptoms of craniofacial lesions result from their expansile nature [33].

CT images show expansile lesions with ground-glass opacity that are based in the medullary cavity of the affected bone (Fig. 9).

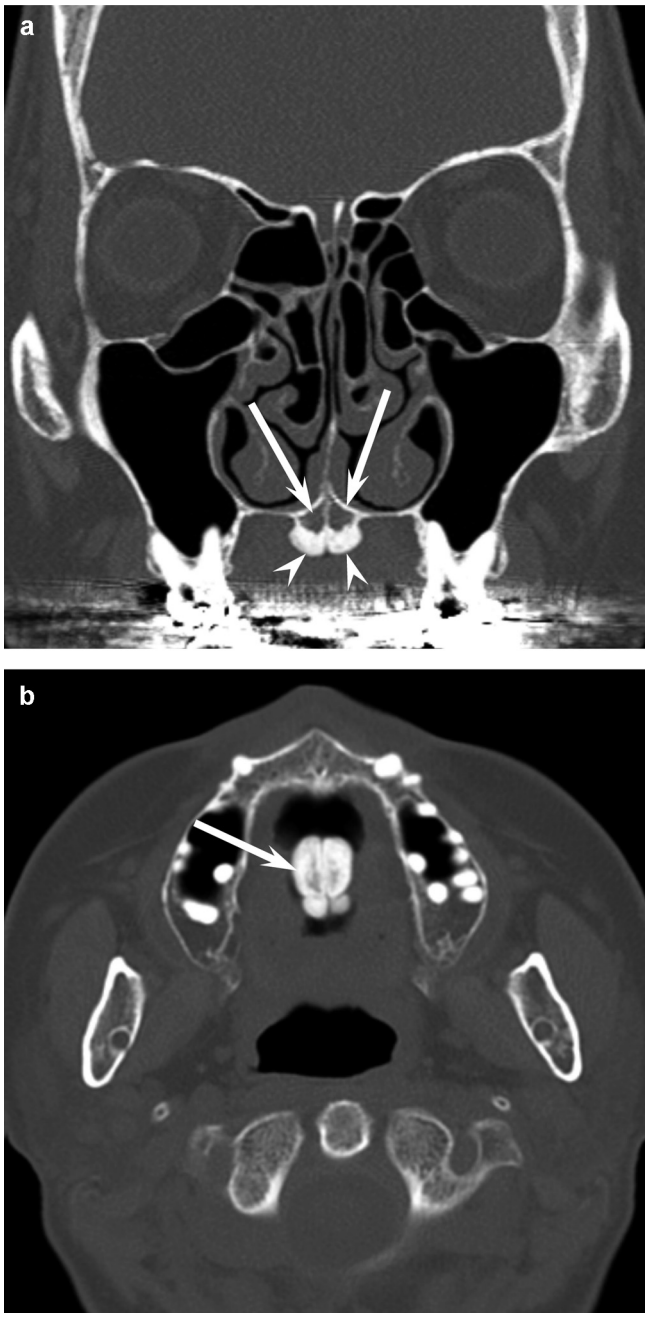

Fig. 8. A 55-year-old woman with Torus palatinus in the midline of the hard palate. (a) Coronal reformatted unenhanced CT image shows a osseous protuberance arising from the hard palate composed of bone marrow (arrows) and compact bone (arrow heads). (b) Axial unenhanced CT image shows a lobulated configuration (arrow).

CT findings of craniofacial lesions show various mixed patterns, including lytic and sclerotic, homogeneously sclerotic, and predominantly cystic or lytic [33]. T2-weighted images show variable and heterogeneous signal patterns due to the proportions of fibrous tissue, mineralized matrix, and cystic components. The cystic components may contain fluid–fluid levels.

5. Malignant tumors

5.1. Adenoid cystic carcinoma

Adenoid cystic carcinoma is the most common salivary gland malignancy in the palate. These tumors typically present as indurated masses in the lateral to middle area of the hard palate and may be ulcerated. Persistent pain usually occurs before any noticeable swelling. Adenoid cystic carcinomas can be classified into three distinct histopathological patterns: tubular, cribriform, and solid [34]. Palatal lesions are known to spread perineurally along the palatine branches of the maxillary nerve [35].

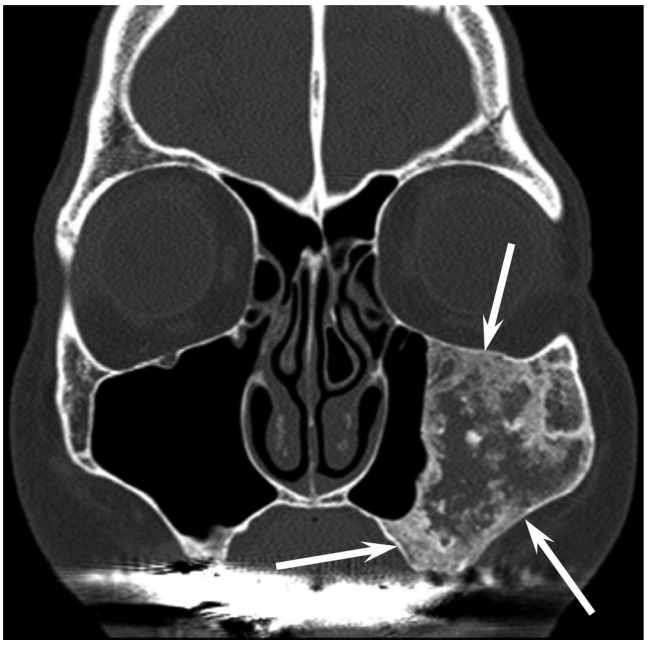

Fig. 9. A 59-year-old woman with fibrous dysplasia of the left maxillary bone and hard palate. Coronal reformatted unenhanced CT image shows a well-demarcated, expansile bone lesion (arrows) with mixed pattern of lytic and sclerotic changes.

Adenoid cystic carcinoma can appear either as a benign or malignant lesion on imaging (Fig. 10a). High-grade tumors have a proclivity to show destructive growth and invasion of the underlying bone. On T2-weighted images, high-grade tumors show hypointensity due to high cellularity, whereas low-grade tumors show hyperintensity due to low cellularity (Fig. 10b) [34]. Palatal lesions frequently demonstrate perineural spread along the greater and lesser palatine nerves, followed by extension to the pterygopalatine fossa and cavernous sinus (Fig. 10c) [35].

5.2. Mucoepidermoid carcinoma

Mucoepidermoid carcinoma is the most common salivary gland malignancy. The palate is the second-most common site, after by the parotid gland. In the oral cavity, these tumors can also be found in the retromolar region, floor of the mouth, lips, and buccal mucosa [36]. Mucoepidermoid carcinomas usually present as painless, slow-growing, reddish-blue, fixed swellings [36]. These tumors are pathologically classified as low-, intermediate-, and high-grade subtypes.

CT and MR images indicate benign or malignant appearances relative to the pathological tumor grade (Fig. 11a). Low-grade tumors have smooth margins and are characterized by mucin-containing cystic components, which appear as hyperintense spots on T1- and T2-weighted images (Fig. 11b) [37]. High-grade tumors tend to be rather solid with poorly defined margins, and they invade the nasal cavity and pterygopalatine fossa and consequently destroy the hard palate and pterygoid plates [36]. High-grade tumors often present as hypo- or isointense lesions on T2-weighted images, indicating their high cellularity.

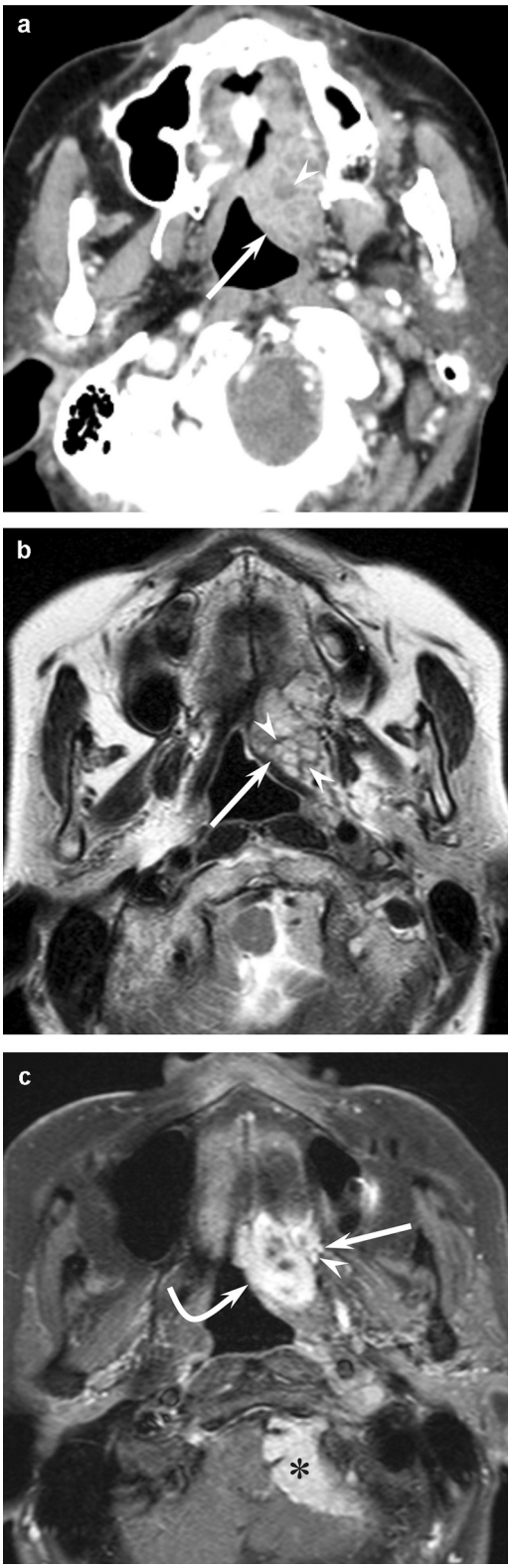

Fig. 10. A 76-year-old woman with adenoid cystic carcinoma of the left hard and soft palate. (a) Axial enhanced CT image shows a heterogeneously enhanced lesion (arrow) with unenhanced cystic components (arrow head). (b) Axial T2-weighted image shows a multicystic appearance (arrow) with septal-like hypointense areas (arrow heads). (c) Axial gadolinium-enhanced fat-suppressed T1-weighted image shows enhanced lesion (curved arrow) with perineural spread into the greater (arrow) and lesser (arrow head) palatine foramen. Left cerebellopontine meningioma is also observed (asterisk).

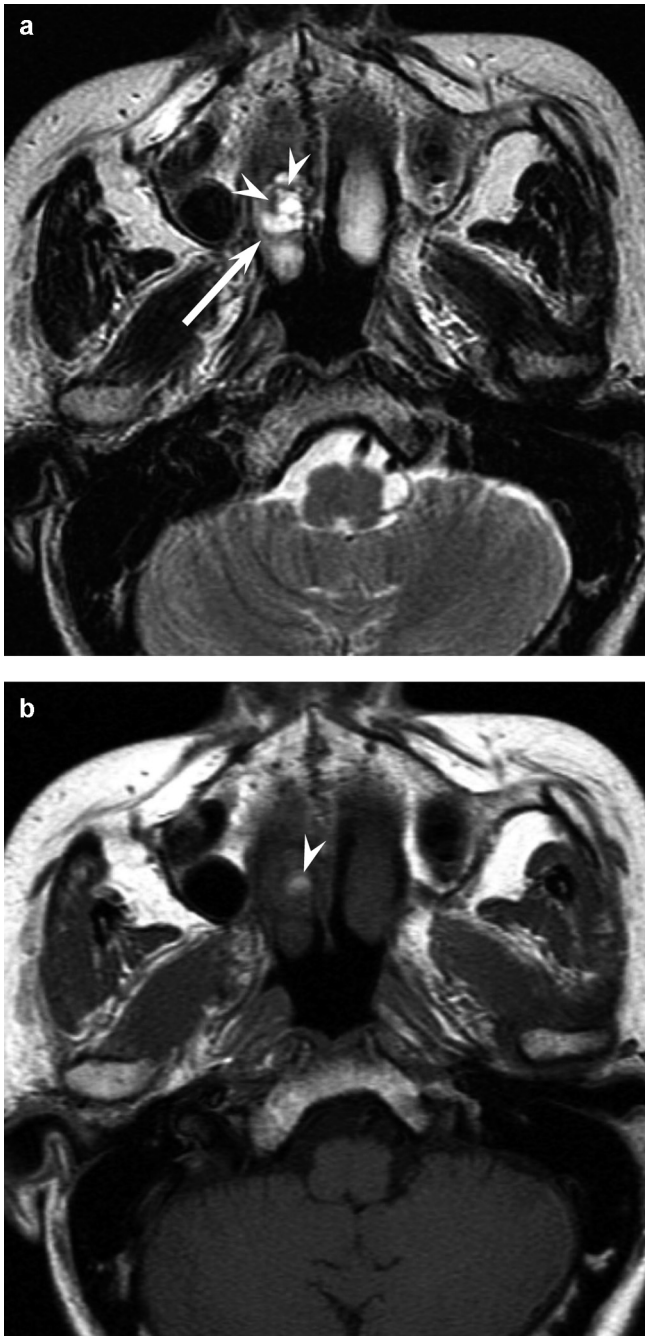

Fig. 11. A 68-year-old woman with mucoepidermoid carcinoma of the right hard palate. (a) Axial T2-weighted image shows a well-demarcated, multicystic lesion (arrow) with septal-like hypointense areas (arrow heads). (b) Axial T1-weighted image shows a focal hyperintense area (arrow head) corresponded with mucin.

5.3. Acinic cell carcinoma

Acinic cell carcinoma is an uncommon low-grade malignancy of the salivary glands. Although most cases occur in the parotid gland, the minor salivary glands, including those in the hard palate, are rarely affected [38]. These tumors usually present as painless, slow-growing masses. Acinic cell carcinomas are histopathologically subdivided into four patterns: solid, microcystic, papillary-cystic, and follicular.

The imaging findings are nonspecific, and most acinic cell carcinomas have a generally benign appearance, often resembling pleomorphic adenoma (Fig. 12) [38,39]. Because microcysts,

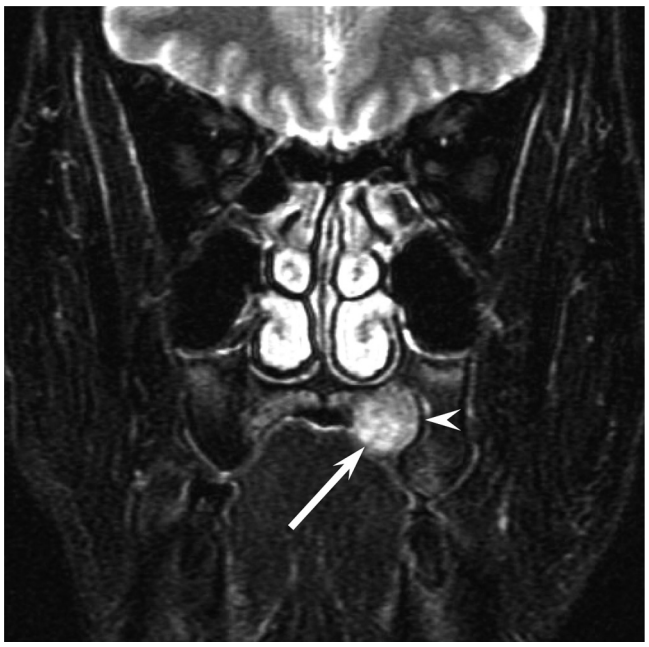

Fig. 12. A 55-year-old man with acinic cell carcinoma of the left hard palate. Coronal fat-suppressed T2-weighted image shows a well-demarcated, heterogenous, hyperintense lesion (arrow) with bone erosion of adjacent maxillary bone (arrow head).

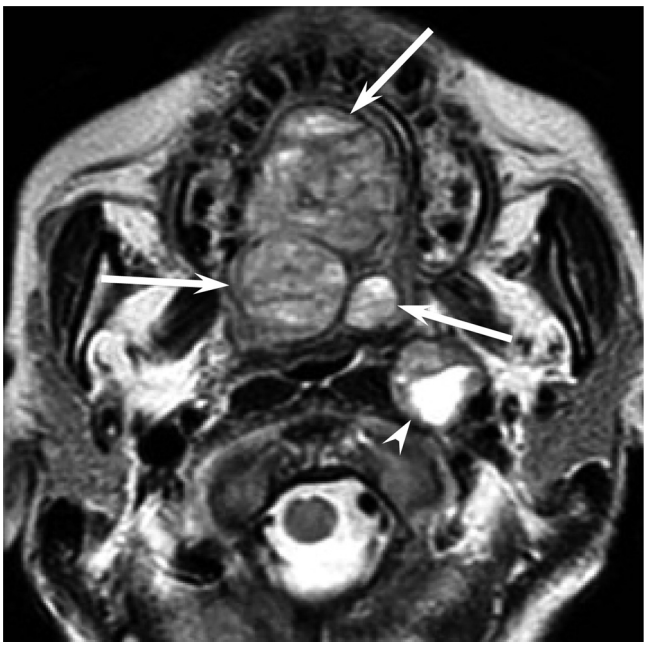

Fig. 13. A 50-year-old woman with polymorphous low-grade adenocarcinoma of the whole palate. Axial T2-weighted image shows a heterogeneous, mixed iso- to hyperintense lesion (arrows). Metastasis to the left retropharyngeal node is found (arrow head).

irregular cystic spaces, hemorrhage, or necrosis are often confirmed during pathologic examinations, intratumoral cystic components are occasionally observed on contrast-enhanced CT Images [38]. Therefore, CT findings are classified into three patterns: solid mass, cystic mass with mural nodule, and cystic mass [38].

5.4. Polymorphous low-grade adenocarcinoma (PLGA)

PLGA is a rare type of salivary gland malignancy found almost exclusively in the minor salivary glands. The most common site is the hard or soft palate, followed by the lips, tongue, buccal mucosa, and floor of the mouth [40]. These tumors frequently manifest as asymptomatic, slow-growing masses that are covered by nonulcerated mucosa, and their clinical behavior resembles that of benign tumors.

The imaging features of PLGA are nonspecific. PLGA can potentially cause bone resorption, medullary infiltration, and invasion of nearby nerves and blood vessels (Fig. 13) [41]. Advanced tumors often extend to the maxillary sinus, nasal cavity, and oropharynx and are accompanied by extensive hard palate bone destruction [40]. CT and MR imaging may be helpful in determining the extent of the tumor in order to provide appropriate management.

5.5. Squamous cell carcinoma (SCC)

The majority of malignancies arising from the soft palate are SCCs, although SCCs of the soft palate are much less common than those of the tonsil or tongue base. In contrast, SCCs rarely arise from the hard palate. SCCs of the soft palate often present as painful and ulcerative masses that can cause dysphagia.

When SCCs are found in the palate, osseous involvement and perineural spread should be carefully evaluated (Fig. 14) [42]. SCCs of the hard palate may extend laterally to invade the maxillary alveolar ridge or superiorly to involve the nasal cavity and maxillary sinuses [42]. Palatal SCCs can spread along the greater and lesser palatine nerves, which provide an upward pathway to the pterygopalatine fossa [42,43]. Perineural spread should be suspected in cases with asymmetric enlargement of the greater or lesser palatine foramen.

5.6. Malignant lymphoma

Malignant lymphoma of the oral cavity is an uncommon pathology. Approximately 20% of oral non-Hodgkin lymphomas occur in the palate [44]. These tumors commonly arise at the junction of the hard and soft palate. Lymphomas usually appear as painless submucosal masses without mucosal ulceration and are

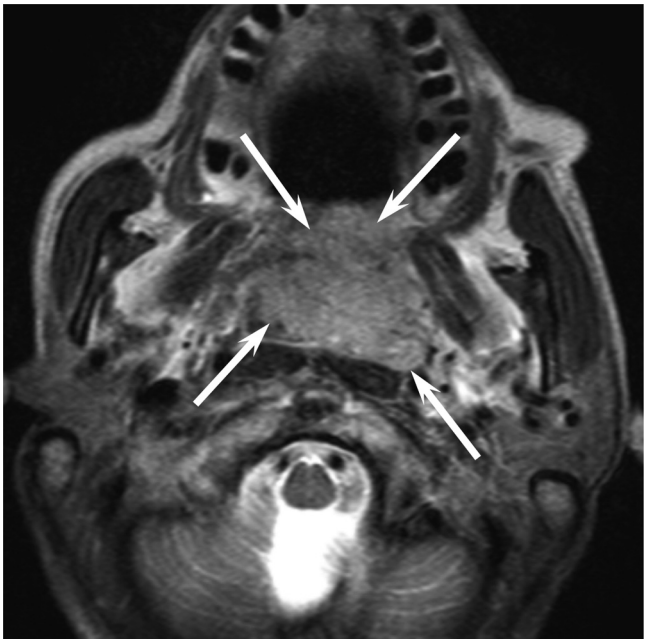

Fig. 14. A 82-year-old man with squamous cell carcinoma of the soft palate. Axial T2-weighted image shows a homogeneously isointense lesion (arrows) with an exophytic growth into the pharyngeal cavity.

Fig. 15. A 53-year-old man with diffuse large B-cell lymphoma of the soft palate. Axial enhanced CT image shows a homogeneous, slightly enhanced lesion (arrows) with an exophytic growth into the pharyngeal cavity.

often accompanied by cervical lymphadenopathy. The common histopathological subtypes of palatal lymphoma are B-cell non-Hodgkin lymphomas, including diffuse large B-cell lymphoma (DLBCL) and mucosa-associated lymphoid tissue (MALT).

Lymphomas that arise from the palate can present either an expansile or destructive growth pattern (Fig. 15). Contrast-enhanced CT and MR images typically show diffuse homogeneous enhancement. On T2-weighted images, these tumors typically appear as homogeneous, slightly hyperintense to isointense masses. On diffusion-weighted images, lymphomas often show smaller apparent diffusion coefficient (ADC) values because of their high cellularity and high nuclear-to-cytoplasm ratio [45].

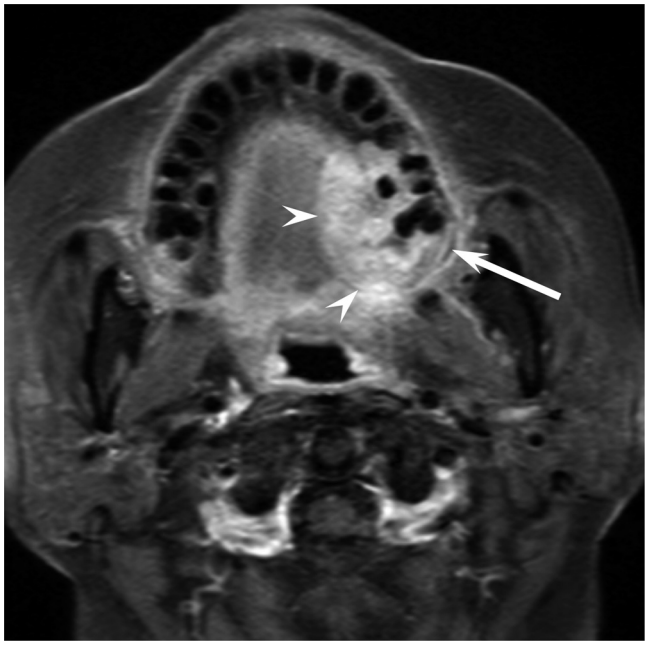

Fig. 16. A 69-year-old woman with left gingival carcinoma. Axial gadolinium-enhanced fat-suppressed T1-weighted image shows a left gingival lesion (arrow) with extension to the left hard palate (arrow heads).

5.7. Secondary tumors

Secondary SCCs of the hard palate often represent extensions from adjacent maxillary gingival SCCs (Fig. 16) [42]. SCCs arising from the tonsils, particularly the anterior tonsillar pillar, tend to spread superiorly along the palatoglossus muscle to the hard and soft palate [42]. In tonsillar SCC, an advanced T-stage and soft palate invasion may predict a high risk of contralateral nodal metastasis [46]. Palatal metastases from renal cell carcinoma [47], lung carcinoma [48], and malignant melanoma [49] have been reported.

6. Conclusions

In conclusion, the differential diagnosis of palatal tumors can present a challenging task for radiologists. However, an understanding of benign and malignant tumors that affect the hard and soft palate allows radiologists to make correct diagnoses, and also directs physicians to appropriate clinical diagnoses and treatments.

References

[1] Yousem DM, Chalian AA. Oral cavity and pharynx. Radiol Clin North Am 1998;36(5):967–81, vii.
[2] Li Q, Zhang XR, Liu XK, et al. Long-term treatment outcome of minor salivary gland carcinoma of the hard palate. Oral Oncol 2012;48(5):456–62.
[3] Yorozu A, Sykes AJ, Slevin NJ. Carcinoma of the hard palate treated with radiotherapy: a retrospective review of 31 cases. Oral Oncol 2001;37(6):493–7.
[4] Al-Abri R, Kumar S, Al-Sudairi S. A palatal mass. Oman Med J 2010;25(1):55–6.
[5] Gandhi D, Gujar S, Mukherji SK. Magnetic resonance imaging of perineural spread of head and neck malignancies. Top Magn Reson Imaging 2004;15(2):79–85.
[6] Chong VF, Fan YF, Khoo JB. MRI features of cervical nodal necrosis in metastatic disease. Clin Radiol 1996;51(2):103–9.
[7] Curtin HD, Ishwaran H, Mancuso AA, Dalley RW, Caudry DJ, McNeil BJ. Comparison of CT and MR imaging in staging of neck metastases. Radiology 1998;207(1):123–30.
[8] King AD, Tse GM, Ahuja AT, et al. Necrosis in metastatic neck nodes: diagnostic accuracy of CT, MR imaging, and US. Radiology 2004;230(3):720–6.
[9] Sumi M, Kimura Y, Sumi T, Nakamura T. Diagnostic performance of MRI relative to CT for metastatic nodes of head and neck squamous cell carcinomas. J Magn Reson Imaging 2007;26(6):1626–33.
[10] Varghese BT, Sebastian P, Abraham EK, Mathews A. Pleomorphic adenoma of minor salivary gland in the parapharyngeal space. World J Surg Oncol 2003;1(1):2.
[11] Rahnama M, Orzedala-Koszel U, Czupkallo L, Lobacz M. Pleomorphic adenoma of the palate: a case report and review of the literature. Contemp Oncol (Pozn) 2013;17(1):103–6.
[12] Feinmesser R, Gay I. Pleomorphic adenoma of the hard palate: an invasive tumour? J Laryngol Otol 1983;97(12):1169–71.
[13] Kakimoto N, Gamoh S, Tamaki J, Kishino M, Murakami S, Furukawa S. CT and MR images of pleomorphic adenoma in major and minor salivary glands. Eur J Radiol 2009;69(3):464–72.
[14] Lev MH, Khanduja K, Morris PP, Curtin HD. Parotid pleomorphic adenomas: delayed CT enhancement. AJNR Am J Neuroradiol 1998;19(10):1835–9.
[15] Kim HS, Lee WM, Choi SM. Myoepitheliomas of the soft palate: helical CT findings in two patients. Korean J Radiol 2007;8(6):552–5.
[16] Barnes L, Appel BN, Perez H, El-Attar AM. Myoepithelioma of the head and neck: case report and review. J Surg Oncol 1985;28(1):21–8.
[17] Wang S, Shi H, Wang L, Yu Q. Myoepithelioma of the parotid gland: CT imaging findings. AJNR Am J Neuroradiol 2008;29(7):1372–5.
[18] Hiwatashi A, Matsumoto S, Kamoi I, Yamashita H, Nakashima A. Imaging features of myoepithelioma arising from the hard palate. A case report. Acta Radiol 2000;41(5):417–9.
[19] Kuribayashi A, Imaizumi A, Tetsumura A, Yoshino N, Kurabayashi T. Magnetic resonance imaging of myoepithelioma in the salivary glands. Oral Radiol 2013;29(1):87–91.
[20] Abbey LM, Page DG, Sawyer DR. The clinical and histopathologic features of a series of 464 oral squamous cell papillomas. Oral Surg Oral Med Oral Pathol 1980;49(5):419–28.
[21] Syrjanen S, Puranen M. Human papillomavirus infections in children: the potential role of maternal transmission. Crit Rev Oral Biol Med 2000;11(2):259–74.
[22] Wright BA, Jackson D. Neural tumors of the oral cavity. A review of the spectrum of benign and malignant oral tumors of the oral cavity and jaws. Oral Surg Oral Med Oral Pathol 1980;49(6):509–22.

[23] Lopez-Carriches C, Baca-Perez-Bryan R, Montalvo-Montero S. Schwannoma located in the palate: clinical case and literature review. Med Oral Patol Oral Cir Bucal 2009;14(9):e465–8.
[24] Kato H, Kanematsu M, Ohno T, et al. Is black geode sign a characteristic MRI finding for extracranial schwannomas? J Magn Reson Imaging 2013;37(4):830–5.
[25] Mulliken JB, Glowacki J. Hemangiomas and vascular malformations in infants and children: a classification based on endothelial characteristics. Plast Reconstr Surg 1982;69(3):412–22.
[26] Gill JS, Gill S, Bhardwaj A, Grover HS. Oral haemangioma. Case Rep Med 2012;2012:347939.
[27] Vilanova JC, Barcelo J, Smirniotopoulos JG, et al. Hemangioma from head to toe: MR imaging with pathologic correlation. Radiographics 2004;24(2):367–85.
[28] Lee DG, Lee SK, Chang HW, et al. CT features of lobular capillary hemangioma of the nasal cavity. AJNR Am J Neuroradiol 2010;31(4):749–54.
[29] Amirchaghmaghi M, Falaki F, Mohtasham N, Mozafari PM. Extragingival pyogenic granuloma: a case report. Cases J 2008;1(1):371.
[30] Kamishima T, Hasegawa A, Kubota KC, et al. Intravenous pyogenic granuloma of the finger. Jpn J Radiol 2009;27(8):328–32.
[31] Garcia-Garcia AS, Martinez-Gonzalez JM, Gomez-Font R, Soto-Rivadeneira A, Oviedo-Roldan L. Current status of the torus palatinus and torus mandibularis. Med Oral Patol Oral Cir Bucal 2010;15(2):e353–60.
[32] Yonetsu K, Nakamura T. CT of calcifying jaw bone diseases. AJR Am J Roentgenol 2001;177(4):937–43.
[33] Lisle DA, Monsour PA, Maskiell CD. Imaging of craniofacial fibrous dysplasia. J Med Imaging Radiat Oncol 2008;52(4):325–32.
[34] Sigal R, Monnet O, de Baere T, et al. Adenoid cystic carcinoma of the head and neck: evaluation with MR imaging and clinical-pathologic correlation in 27 patients. Radiology 1992;184(1):95–101.
[35] Shimamoto H, Chindasombatjaroen J, Kakimoto N, Kishino M, Murakami S, Furukawa S. Perineural spread of adenoid cystic carcinoma in the oral and maxillofacial regions: evaluation with contrast-enhanced CT and MRI. Dentomaxillofac Radiol 2012;41(2):143–51.
[36] Herd MK, Murugaraj V, Ghataura SS, Brennan PA, Anand R. Low-grade mucoepidermoid carcinoma of the palate—a previously unreported case of metastasis to the liver. J Oral Maxillofac Surg 2012;70(10):2343–6.
[37] Okahara M, Kiyosue H, Hori Y, Matsumoto A, Mori H, Yokoyama S. Parotid tumors: MR imaging with pathological correlation. Eur Radiol 2003;13(Suppl. 4):L25–33.
[38] Suh SI, Seol HY, Kim TK, et al. Acinic cell carcinoma of the head and neck: radiologic–pathologic correlation. J Comput Assist Tomogr 2005;29(1):121–6.
[39] Sakai O, Nakashima N, Takata Y, Furuse M. Acinic cell Carcinoma of the parotid gland: CT and MRI. Neuroradiology 1996;38(7):675–9.
[40] Gonzalez-Garcia R, Rodriguez-Campo FJ, Munoz-Guerra MF, Nam-Cha SH, Sastre-Perez J, Naval-Gias L. Polymorphous low-grade adenocarcinoma of the palate: report of cases. Auris Nasus Larynx 2005;32(3):275–80.
[41] Seethala RR, Johnson JT, Barnes EL, Myers EN. Polymorphous low-grade adenocarcinoma: the University of Pittsburgh experience. Arch Otolaryngol Head Neck Surg 2010;136(4):385–92.
[42] Trotta BM, Pease CS, Rasamny JJ, Raghavan P, Mukherjee S. Oral cavity and oropharyngeal squamous cell cancer: key imaging findings for staging and treatment planning. Radiographics 2011;31(2):339–54.
[43] Beil CM, Keberle M. Oral and oropharyngeal tumors. Eur J Radiol 2008;66(3):448–59.
[44] Kemp S, Gallagher G, Kabani S, Noonan V, O'Hara C. Oral non-Hodgkin's lymphoma: review of the literature and World Health Organization classification with reference to 40 cases. Oral Surg Oral Med Oral Pathol Oral Radiol Endod 2008;105(2):194–201.
[45] Kato H, Kanematsu M, Kawaguchi S, Watanabe H, Mizuta K, Aoki M. Evaluation of imaging findings differentiating extranodal non-Hodgkin's lymphoma from squamous cell carcinoma in naso- and oropharynx. Clin Imaging 2013;37(4):657–63.
[46] Lee DJ, Kwon MJ, Nam ES, et al. Histopathologic predictors of lymph node metastasis and prognosis in tonsillar squamous cell carcinoma. Korean J Pathol 2013;47(3):203–10.
[47] Kohli M, Schaefer R. Management of solitary palatal metastasis from renal cell carcinoma. Nat Clin Pract Urol 2006;3(7):6–392 [quiz following 6].
[48] Piattelli A, Tamborrino F. Soft palate metastasis from a small cell carcinoma of the lung. Acta Stomatol Belg 1995;92(1):31–3.
[49] Ram H, Mohammad S, Husain N, Devi S, Gupta PN. Metastatic malignant melanoma of palate: a review of literature and report of an unusual case. Natl J Maxillofac Surg 2010;1(1):63–6.